PeAPA | Publicación Electrónica
ASOCIACIÓN PALEONTOLÓGICA ARGENTINA

www.peapaleontologica.org.ar

Geochemical signals in Paleogene penguins from Seymour Island (Isla Marambio), Antarctic Peninsula

LEANDRO MARTÍN PÉREZ[1,6,7]
CAROLINA ACOSTA HOSPITALECHE[2,6,7]
LUCÍA ELENA GÓMEZ-PERAL[3,6,7]
ALEJANDRO GÓMEZ DACAL[4,6,7]
MARCELO ALFREDO REGUERO[2,5,7]
DANIEL GUSTAVO POIRÉ[3,6,7]
CLAUDIA ERNESTINA CAVAROZZI[3,6,7]

1. División Paleozoología Invertebrados, Museo de La Plata, Universidad Nacional de La Plata (UNLP). Paseo del Bosque s/n, 1900 La Plata, Buenos Aires, Argentina.
2. División Paleontología de Vertebrados, Museo de La Plata, Universidad Nacional de La Plata (UNLP). Paseo del Bosque s/n, 1900 La Plata, Buenos Aires, Argentina.
3. Centro de Investigaciones Geológicas (CIG)-Consejo Nacional de Investigaciones Científicas y Técnicas (CONICET)-Universidad Nacional de La Plata (UNLP). Diagonal 113 y 64, 1900 La Plata, Buenos Aires, Argentina.
4. YPF Tecnología S.A. (Y-TEC). Avenida del Petróleo Argentino 900-1198, 1923 Berisso, Buenos Aires, Argentina.
5. Instituto Antártico Argentino (IAA), Dirección Nacional del Antártico (DNA). Balcarce 295, C1064AAF Ciudad Autónoma de Buenos Aires, Argentina.
6. Facultad de Ciencias Naturales y Museo (FCNyM), Universidad Nacional de La Plata (UNLP). Avenida 122 y 60, 1900 La Plata, Buenos Aires, Argentina.
7. Consejo Nacional de Investigaciones Científicas y Tecnológicas (CONICET). Godoy Cruz 2290, C1425FQB Ciudad Autónoma de Buenos Aires, Argentina.

Recibido: 16 de septiembre 2022 - **Aceptado:** 14 de noviembre 2022 - **Publicado:** 22 de febrero 2023

Para citar este artículo: Leandro Martín Pérez, Carolina Acosta Hospitaleche, Lucía Elena Gómez-Peral, Alejandro Gómez Dacal, Marcelo Alfredo Reguero, Daniel Gustavo Poiré, & Claudia Ernestina Cavarozzi (2023). Geochemical signals in Paleogene penguins from Seymour Island (Isla Marambio), Antarctic Peninsula. *Publicación Electrónica de la Asociación Paleontológica Argentina* 23 (1): 18–33.

Link a este artículo: http://dx.doi.org/10.5710/PEAPA.14.11.2022.443

ISSN 2469-0228

Asociación Paleontológica Argentina
Maipú 645 1° piso, C1006ACG, Buenos Aires
República Argentina
Tel/Fax (54-11) 4326-7563
Web: www.apaleontologica.org.ar

Publicación Electrónica
ASOCIACIÓN PALEONTOLÓGICA ARGENTINA
Año 2023 - 23(1): 18–33
ARTÍCULO

GEOCHEMICAL SIGNALS IN PALEOGENE PENGUINS FROM SEYMOUR ISLAND (ISLA MARAMBIO), ANTARCTIC PENINSULA

LEANDRO MARTÍN PÉREZ[1,6,7], CAROLINA ACOSTA HOSPITALECHE[2,6,7], LUCÍA ELENA GÓMEZ-PERAL[3,6,7], ALEJANDRO GÓMEZ DACAL[4,6,7], MARCELO ALFREDO REGUERO[2,5,7], DANIEL GUSTAVO POIRÉ[3,6,7], AND CLAUDIA ERNESTINA CAVAROZZI[3,6,7]

[1]División Paleozoología Invertebrados, Museo de La Plata, Universidad Nacional de La Plata (UNLP). Paseo del Bosque s/n, 1900 La Plata, Buenos Aires, Argentina. *pilosaperez@gmail.com*

[2]División Paleontología de Vertebrados, Museo de La Plata, Universidad Nacional de La Plata (UNLP). Paseo del Bosque s/n, 1900 La Plata, Buenos Aires, Argentina. *acostacaro@fcnym.unlp.edu.ar*; *regui@fcnym.unlp.edu.ar*

[3]Centro de Investigaciones Geológicas (CIG)-Consejo Nacional de Investigaciones Científicas y Técnicas (CONICET)-Universidad Nacional de La Plata (UNLP). Diagonal 113 y 64, 1900 La Plata, Buenos Aires, Argentina. *luciagomezperal@gmail.com*; *dgpoire@yahoo.com.ar*; *cavarozzi@cig.museo.unlp.edu.ar*

[4]YPF Tecnología S.A. (Y-TEC). Avenida del Petróleo Argentino 900-1198, 1923 Berisso, Buenos Aires, Argentina. *agomezdacal@gmail.com*

[5]Instituto Antártico Argentino (IAA), Dirección Nacional del Antártico (DNA). Balcarce 295, C1064AAF Ciudad Autónoma de Buenos Aires, Argentina.

[6]Facultad de Ciencias Naturales y Museo (FCNyM), Universidad Nacional de La Plata (UNLP). Avenida 122 y 60, 1900 La Plata, Buenos Aires, Argentina.

[7]Consejo Nacional de Investigaciones Científicas y Tecnológicas (CONICET). Godoy Cruz 2290, C1425FQB Ciudad Autónoma de Buenos Aires, Argentina.

LMP: https://orcid.org/0000-0003-4038-1859; **CAH:** https://orcid.org/0000-0002-2614-1448; **LEGP:** https://orcid.org/0000-0002-6303-6604; **AGD:** https://orcid.org/0000-0002-9466-7580; **MAR:** https://orcid.org/0000-0003-0875-8484; **DGP:** https://orcid.org/00000-0003-0966-122X; **CEC:** https://orcid.org/0000-0001-9862-1646

Abstract. Trace elements, particularly rare earth elements (REE), are widely used as proxies to reconstruct paleoenvironmental and taphonomic conditions. We traced these elements in fossil penguin bones collected along the Paleogene sequence exposed in Seymour Island (=Isla Marambio) to test them as indicators of the tectonic changes to which this region was exposed. The results indicated the contents of REE in thirteen samples of the analyzed bone tissues. The negative europium anomaly in the samples from Bartonian and Priabonian beds reflects regional events. This signal coincides in time with the opening of the Drake Passage, and with the tectonic changes that occurred between the end of the Eocene and the beginning of the Oligocene, between the western margin of South America and the Antarctic Peninsula.

Key words. Sphenisciformes. ICP-MS analysis. Fossil-diagenesis. Taphonomy. Weddell sea. Antarctica.

Resumen. SEÑALES GEOQUÍMICAS EN PINGÜINOS DEL PALEÓGENO DE ISLA MARAMBIO (SEYMOUR ISLAND), PENÍNSULA ANTÁRTICA. Los elementos traza, y particularmente los Elementos de las Tierras Raras (REE por sus siglas en inglés), son ampliamente utilizados como indicadores para la reconstrucción de condiciones paleoambientales y tafonómicas. Rastreamos estos elementos en huesos fósiles de pingüinos recolectados a lo largo de la secuencia del Paleógeno expuestos en la Isla Marambio (=Seymour Island) para testearlos como indicadores de los cambios tectónicos a los que estuvo expuesta la región. Los resultados indicaron las concentraciones de REE en el interior de las trece muestras de tejido óseo analizado. La anomalía de europio negativa en las muestras de nivel Bartoniano y Priaboniano refleja eventos regionales. Esta señal coincide en el tiempo con la apertura del Pasaje de Drake, y con los cambios tectónicos que ocurrieron entre finales del Eoceno y principios del Oligoceno, entre el margen occidental de las costas de América del Sur y la Península Antártica.

Palabras clave. Sphenisciformes. Análisis ICP-MS. Fosildiagénesis. Tafonomía. Mar de Weddell. Antártida.

THE UNDERSTANDING of the mechanisms and distribution of trace element uptake in bioapatite sparks widespread scientific interest (Decrée *et al.*, 2018). In this sense, trace elements—and particularly REE—are widely used as proxies for paleoenvironment, taphonomy, provenance, and also to reveal paleoceanographic controls (*e.g.*, Trueman & Tuross, 2002; Trueman *et al.*, 2006; Herwartz *et al.*, 2011). In addition, REE patterns in fossil biogenic apatite are often interpreted to reflect those of the early diagenetic ambient seawater or pore fluid, insofar as typical aqueous REE patterns are preserved (Herwartz *et al.*, 2011). Low $(La/Sm)_N$ ratios, for instance, have been used as one criterion indicating late diagenetic recrystallization of biogenic apatite (*e.g.*, Reynard *et al.*, 1999; Trueman *et al.*, 2006; Gómez-Peral *et al.*, 2014; Decrée *et al.*, 2018).

Bone apatite acts as a natural, timed sampling device, scavenging trace elements from local pore waters over timescales of *ca.* 1–50 ka. The REE composition of fossil

bones reflects associated pore water compositions during recrystallization. In this case, the geochemical signal preserved in fossil bones allows us to indirectly understand the changes associated with the fossilization occurring in the depositional environment at that moment, in taphonomic processes linked to bone accumulations.

Tracing REE is a relatively new tool for detecting tectonic and paleoceanographic events (Cook & Shergold, 2005). This technique has never been used in Antarctica, where the record of vertebrates represents a unique opportunity to test this kind of proxy. We selected the Paleogene penguins from Seymour Island (=Isla Marambio) (and the species that live in the area today as a *proxy*) for searching REE.

Penguins (Sphenisciformes) are flightless marine birds currently represented by 17 species that live in austral oceans and are associated with cold currents (Williams, 1995). The oldest records of penguins date back to the Paleocene of New Zealand (Slack *et al.*, 2006; Blokland *et al.*, 2019, among others) and Antarctica (Tambussi *et al.*, 2005; Acosta Hospitaleche *et al.*, 2016). All the described species have been recorded in the Southern Hemisphere. The diversity and abundance of the Antarctic record, particularly during the Eocene, made penguins (together with selaceans) the dominant fossil vertebrates of Seymour Island in the AP.

The Eocene record of Antarctic penguins, represented by an almost uninterrupted sequence from the Thanetian to the Rupelian (Acosta Hospitaleche *et al.*, 2013, 2019a), is one of the richest and most diverse in the world. Most of the remains correspond to fragmentary and incomplete bones. Consequently, the systematics of the group is far from being resolved. Nevertheless, the Antarctic penguin record is a practically inexhaustible source of information to carry out different kinds of studies (see for example Presslee *et al.*, 2020). The fossil record of Paleogene penguin bones from Seymour Island is particularly variable, abundant, and continuous throughout the exposed sections. In general, bones appear in large concentrations, although isolated (Acosta Hospitaleche *et al.*, 2019a and references cited there) and articulated specimens have rarely been recorded (*e.g.*, Acosta Hospitaleche & Reguero, 2010, 2014; Acosta Hospitaleche *et al.*, 2019b).

The holotype of *Crossvallia unienwillia* Tambussi *et al.*, 2005, is the only material known from the Paleocene CVF. This skeleton consists of a few associated elements with marked weathering (Acosta Hospitaleche *et al.*, 2016). In the upper levels of the CVF, the amount of materials increases notoriously. In the LMF (Thanetian–Lutetian), remains are scattered and preserved as isolated elements; finally, in the overlying SMF (Lutetian–Rupelian) penguins exhibit a more abundant record, with partially articulated skeletons, skulls, and articulated limbs, including the exceptional record of a wing covered by the phosphatized skin (Acosta Hospitaleche *et al.*, 2020).

In the present contribution, samples were treated as *taxon free* and our attention was focused on the osteological and taphonomical state of the bones. The microstructure of the sampled bones (pachyostosis degree, compactness, and lack of pneumaticity) and their preservation (mineralization, composition, weathering, and completeness) are very similar to each other and, therefore, comparable for our purposes.

The opening process of the Drake Passage, as a large-scale tectonic phenomenon that gave rise to the Antarctic Circumpolar Current, began towards the end of the Eocene (~35 Ma) and the early Oligocene (see Lawver & Gahagan, 2003). This process generated significant changes in climatic and ecological conditions in the biota that inhabited those latitudes, with phenomena of extinctions and compositional changes in the assemblages (Crame *et al.*, 2014). In this changing scenario, penguins, as marine divers, have probably taken advantage of the new opportunities, spreading to new areas. This process culminated in the definitive separation of the Antarctic, Australasian, and South American regions prior to developing the Antarctic Circumpolar Current (Lawver & Gahagan, 2003).

In this context, the main objective of this work is the identification, through geochemical analysis, of trace elements present in penguin bones collected along the Paleogene sequence that outcrops on Seymour Island for the interpretation and linking of the results from a regional depositional, diagenetic, and tectonic fossil significance.

GEOLOGICAL SETTING

Paleogene sequences in Seymour Island

The first stratigraphic studies on Seymour Island were carried out during the Swedish polar expedition 1901–1903 under the command of Dr. Otto Nordenskjöld (Andersson,

1906). After that, various contributions to the subject completed the modern stratigraphic scheme of the outcropping sections on the island, until reaching the current model (*e.g.*, Bibby, 1966; Elliot *et al.*, 1975; Rinaldi *et al.*, 1978; Feldman & Woodbume, 1988; Macellari, 1988; Sadler, 1988). In recent years there has been a constant review of the general geology of the sequences exposed on the island, with several significant contributions (*e.g.*, Marenssi & Elliot, 1992; Marenssi & Santillana, 1994; Marenssi, 1995; Marenssi *et al.*, 1998, 2002; Olivero *et al.*, 2008; Montes *et al.*, 2019).

Seymour Island (Fig. 1.1–3) is composed of the youngest sediments that fill the James Ross Basin, which is considered the northern tip of the Larsen Basin (MacDonald *et al.*, 1988). The sequence exposed on this island is constituted by the Maastrichtian–early Paleocene Marambio Group with the Haslum Crag Formation (*sensu* Olivero *et al.*, 2008), López de Bertodano Formation, and the Sobral Formation (Rinaldi *et al.*, 1978; Montes *et al.*, 2019). Unconformably overlying is the late Paleocene–earliest Oligocene? Seymour Island Group (Zinsmeister, 1982)—the focus of the present study—constituted by the CVF (Cross Valley-Wiman Formation according to Montes *et al.*, 2008), LMF, and the SMF (Submeseta Allomember in Marenssi *et al.*, 1998) (Montes *et al.*, 2013, 2019). A detail of each of them can be found below and in the integrated stratigraphic column (Fig. 1.4).

CVF (late Thanetian). The CVF is approximately 195 m thick (Marenssi *et al.*, 2012), unconformably underlying the LMF, outcropping in two different sectors in Seymour Island. The main lithology is a sedimentary succession of sandstone of massive character, dark clays, with a high content of volcanic lithic fragments, abundant charred trunks, and few macro-fossil in the upper part of the section. This formation was divided into three allomembers, *i.e.*, Cross Valley A or Díaz Allomember, Cross Valley B or Arañado Allomember, and Cross Valley C or BP Allomember (Montes *et al.*, 2007, 2019).

The Díaz Allomember is interpreted as the filling of paleochannels with onlap geometry, with an upper erosive bounding surface (Montes *et al.*, 2007). The Arañado Allomember outcrops generate a great relief change due to increased in sediment grain size of paleochannel fills and increased lithification. Finally, the BP Allomember is the thinnest among these three levels, with an approximate maximum of 20 m and is composed at its base of gray mudstones containing oysters, gastropods, echinoderms, fish teeth, sharks, and penguins (Tambussi *et al.*, 2005; Montes *et al.*, 2007). Indeed, these deposits turn to a more siliciclastic composition to the detriment of the volcanic elements. The outcrops of the Cañadón Díaz area, where the samples analyzed here were collected, present a morphology also consistent with channels (Montes *et al.*, 2019).

The whole deposits of the CVF correspond to a shallow succession which constitutes an aggradational or a progradational system during a transgressive system. It might represent an estuarine environment, concluding with deltaic facies (Elliot & Trautman, 1982). According to the latest studies, the CVF is interpreted as a strongly incised valley developed over a previously emerged platform (Montes *et al.*, 2019).

LMF (Ypresian–early Lutetian). This unit unconformably overlies the CVF, filling an incised valley in a passive margin platform (Montes *et al.*, 2019). It is formed mainly by a detrital series including breccia, sandstone, and shale with accumulation horizons of mollusk shells (Montes *et al.*, 2019). This unit is internally subdivided into six allomembers known as Valle de las Focas, Acantilados I, Acantilados II (both Acantilados I and II correspond to Acantilados *sensu* Marenssi *et al.*, 1998), Campamento, Cucullaea I, and Cucullaea II (Montes *et al.*, 2013, 2019). The whole sequence represents prodeltaic, deltaic, and especially estuarine depositional environments dominated by tides. Sea-level variations and the source area of the deposits controlled the evolution of these environments (Marenssi, 1995; Marenssi *et al.*, 2002).

The Valle de las Focas Allomember (unit 31) is interpreted as the collapse of the incised valley edges and sedimentation in a low-energy environment (Montes *et al.*, 2019). The Acantilados I Allomember (unit 32) was deposited under fluctuating energy conditions in a tide-dominated marine environment below wave base level (Marenssi, 1995). The Acantilados II Allomember (unit 33) would result from a deltaic front prograding onto a tide-dominated platform influenced by storms (Montes *et al.*, 2019). The Campamento Allomember (unit 34) was deposited during a drop in the relative sea level, filling the canal after the erosion and collapse of the canal margins.

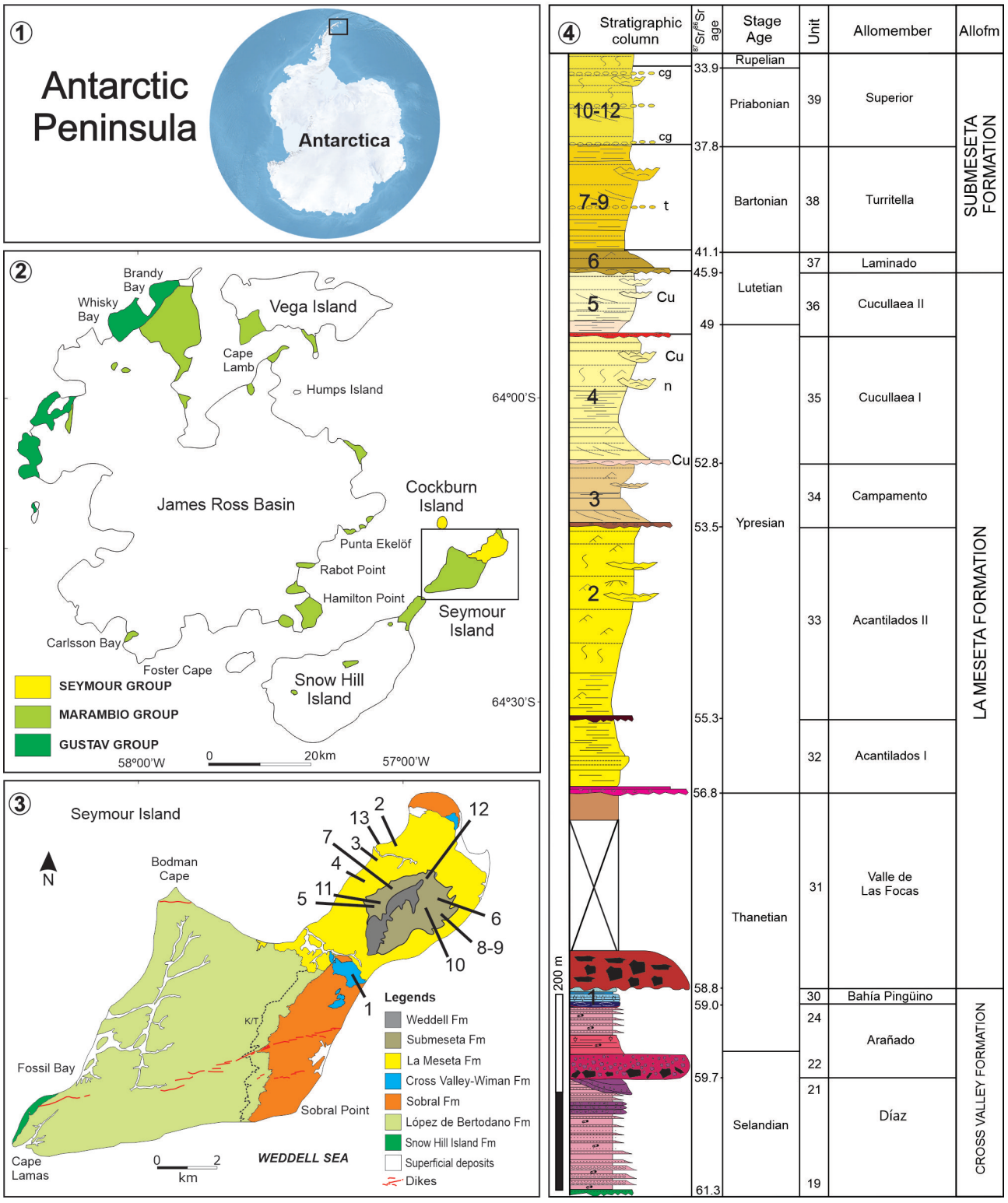

Figure 1. 1–4, Location map and stratigraphic column of the collection area (modified from Montes *et al.*, 2019); **1,** Location map of the study area at the Seymour Island, in the **AP**; **2,** James Ross Basin, the square indicates the Seymour Island; **3,** Map showing outcrops of the Seymour Island; **4,** Stratigraphic column with the location of the samples analyzed in the present paper, indicated with the numbers 1–12. Abbreviations: **Allofm,** Alloformation; **cu,** *Cucullaea*; **cg,** conglomerates; **Fm,** Formation; **t,** *Turritella;* **n,** naticids.

This unit shows sectors with more protected environments characterized by a low re-sedimentation and a rapid burial, others of subtidal environments with an intense reworking made by waves and currents, and tidal infill facies with a general transgressive tendency (Montes *et al.*, 2019). The overlying Cucullaea I Allomember represents a subtidal environment with a moderate reworking of the substrate provoked by waves and currents, with a deltaic front over muddy pro-deltaic deposits (Marenssi, 1995; Montes *et al.*, 2019). Covering canalized facies and within an estuarine environment, a tidal plain establishes coastal environments in a transgressive context (Montes *et al.*, 2019). Finally, the Cucullaea II Allomember sediments are interpreted as tidal deposits within an estuarine context (Montes *et al.*, 2019).

SMF (Lutetian–Priabonian). At the top of the section, and resting unconformably, this unit has been interpreted as storm-dominated shallow-sea platform deposits. It is composed of breccia and conglomerate-like sediments, with beds of coquinas and coarse sandstones with internal structures (Montes *et al.*, 2019). It is internally subdivided into three allomembers known as Laminado (Submeseta I), Turritella (Submeseta II), and Superior (Submeseta III); they represent the incised valley clogging (Montes *et al.*, 2019).

The Laminado Allomember is interpreted as a tidal plain in an estuarine context, whereas the Turritella Allomember would correspond to sandy sediments of a shallow tidal platform with bars and protected areas in-between, with a more distal muddy area. Thus, the depositional environments of these beds change significantly compared with the units below, due to the valley clogging and the establishment of a broad sandy platform where periodic storms are recorded (Montes *et al.*, 2019). A progressive water-cooling would be indicated by the decrease in the number of mollusk shells (Elliot & Trautman, 1982). Finally, at the bottom, the Superior Allomember is also interpreted as a tide-dominated sandy shallow marine platform.

This unit represents a sandy shelf depositional environment with sporadic high-energy events product of tidal currents and storms (Marenssi, 1995; Marenssi *et al.*, 1998). Glacial conditions (Ivany *et al.*, 2006; Warny *et al.*, 2018) and a subpolar climate (Montes *et al.*, 2019) were established at the top of this unit.

Tectonic and paleogeographic framework

The paleogeographical changes due to the continental breakup leading to the separation of Patagonia (including the Magallanes Region) and the AP crustal block began with the opening of the Atlantic Ocean in the Early Cretaceous and running up to the early Paleogene with the expansion of the Scotia Basin (Eagles *et al.*, 2005). All these processes implied two distinct paleogeographic and paleobiogeographic scenarios (before and after their geographic and faunistic isolation) for the evolution of the faunas (West Weddellian Terrestrial Biogeographic Province; Reguero & Goin, 2021).

WANT has formed the tectonically active margin between EANT and the Pacific Ocean for almost half a billion years. It underwent a dynamic history of magmatism, continental growth, and fragmentation. From the Late Cretaceous to the Neogene, the collision of spreading ridge segments (AP and Thurston Island crustal blocks) at the continental ocean boundary triggered the progressive shutdown of subduction along the AP margin from south to north. The arc magmatism declined since the beginning of the Cenozoic (Fig. 2) (Jordan *et al.*, 2020).

The AP and Thurston Island exemplify a continental margin magmatic arc, preserving a record of the flare-ups in magmatism. Arc magmatism ceased northwards between 90 and 20 Ma as the Phoenix oceanic spreading center reached the continental margin trench. Arc magmatism finally ceased on the AP at ~20 Ma in the South Shetland Islands, even though the subduction continues today (Jordan *et al.*, 2020). This ongoing subduction led to rifting along the Bransfield Strait at ~10 Ma, which split the Pacific margin magnetic anomaly and is associated with ongoing alkaline magmatism in the South Shetland Islands (Fretzdorff *et al.*, 2004). Contemporaneous with Cenozoic magmatism, extension between South America and the AP coupled with the back-arc extension of the Scotia subduction zone led to the opening of the Drake Passage at the end of the Eocene and the beginning of the Oligocene. This event enabled the development of the Antarctic Circumpolar Current (see Lawver & Gahagan, 2003; Eagles *et al.*, 2006). Total separation of the land masses occurred during the late Oligocene–early Miocene (*e.g.*, Livermore *et al.*, 2005; Lagabrielle *et al.*, 2009; Eagles & Jokat, 2014). Reguero *et al.* (2014) proposed that the early stages of the extensive

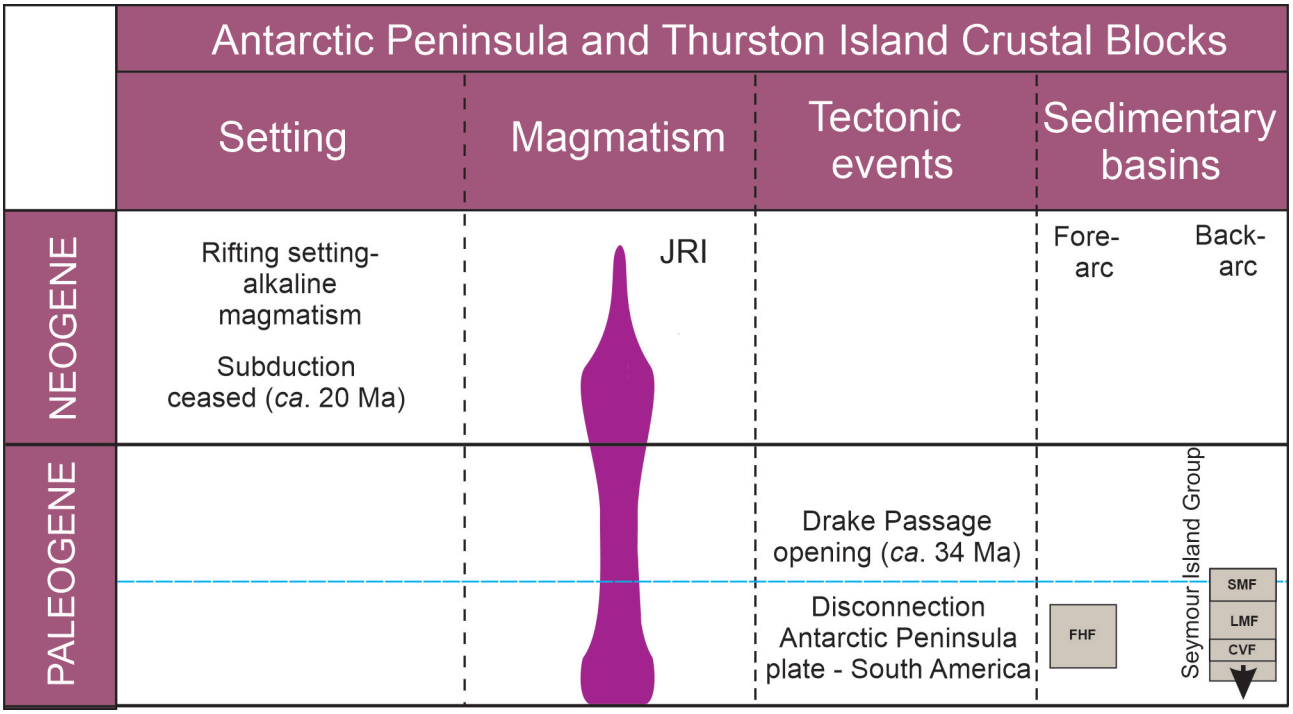

Figure 2. Cenozoic timeline of key West Antarctic tectonic and magmatic events in the **WANT** (**AP** and Thurston Island). The purple band in the 'Magmatism' column shows the relative magnitude of arc-related and rift-related magmatism, respectively (modified from Reguero & Goin, 2021). The light blue line indicates the opening of the Drake Passage time. Abbreviations: **FHF,** Fossil Hill Formation.

Drake Passage opening (late Paleocene, ~55 Ma) generated a wide and relatively shallow epicontinental sea that flooded the Weddellian Isthmus. Such an event was produced by the subduction of the Pacific plates and the development and advance of the Scotia volcanic arc towards the eastern Atlantic sector.

The opening of the Drake Passage would have entailed a reduced heat transport towards the south of ocean currents. The thermal insulation and consequent climatic cooling of Antarctica are the results of these processes (*e.g.*, Toggweiler & Bjornsson, 2000; Sijp & England, 2004).

MATERIAL AND METHODS

Fieldwork. Thirteen samples of recent and fossil penguin bones belonging to adult specimens were collected during successive field trips to Seymour Island (WANT), by members of the IAA and MLP, and are permanently housed at the DPV (in MLP). Twelve samples correspond to fossil penguin bones selected from different levels and localities and the thirteenth one belongs to an extant bone (S13) of *Pygoscelis adeliae* (Hombron & Jacquinot, 1841) collected also in Seymour Island, and analyzed as the control sample (Tab. 1). All the samples were free of glue or any other chemical compound that could generate noise in the results of our analyses.

ICP-MS analysis. A subsample of the innermost part of each fossil-bone was taken to obtain unaltered bioapatite. The samples for ICP-MS analysis were powdered using a Drill-Mets micro-drilling machine avoiding the incorporation of any component of diagenetic origin during the sampling. The powdered subsamples were digested for 2 h in trace metal grade 2% HNO_3 v/v added dropwise, using sufficient acid to dissolve 100% of the apatite. Solutions were centrifuged and decanted to remove insoluble residue. Precision and reproducibility for all elements analyzed are greater than 10%, based on replicate measurements of laboratory apatite standards.

A Perkin-Elmer quadrupole ICP-MS, fitted with a Meinhardt concentric nebulizer from the Centro de Investigaciones Geológicas (Consejo Nacional de Investigaciones Científicas y Técnicas-Universidad Nacional de La Plata, La Plata, Argentina) was used to determine REE and Y concen-

trations in ppm and other traces of elements such as Ba, Mn, and Sr (Tab. 2).

The REE concentrations were normalized to Chondrite values (Sun & McDonough, 1989), plotted in pattern distribution graphics and compared to a geostandard of volcanic rock (RGM-1=acid~rhyolite). REE concentrations were also normalized relative to the PAAS (McLennan, 1989) and represented with the symbol "N". Shale-normalized (N) elemental values were used according to Taylor & McLennan (1985) for the calculation of $(La/Sm)_N$ and $(La/Yb)_N$ ratios and other anomalies calculated on a linear scale, assuming that differences in concentration between neighboring pairs are constant. In addition, cerium anomalies were obtained from the formulae $Ce/Ce^*=2Ce_N/(La_N+Pr_N)$ of De Baar *et al.* (1985). Eu anomaly was also calculated from a geometric average, assuming that the ratio between near neighbor concentrations is constant, as follows: $Eu/Eu^*=Eu_N/(Sm_N x Tb)$ 0.33 following Lawrence *et al.* (2006).

Institutional acronyms. DPV, División Paleontología Vertebrados, Museo de La Plata, Universidad Nacional de La Plata, La Plata, Argentina; **IAA,** Instituto Antártico Argentino, Ciudad Autónoma de Buenos Aires, Argentina; **MLP,** Museo de La Plata, La Plata, Argentina.

Abbreviations. AP, Antarctic Peninsula; **Ba,** barium; **BP,** Bahía Pingüino; **Ce,** cerium; **CVF,** Cross Valley Formation; **Dy,** dysprosium; **Er,** erbium; **Eu,** europium; **Gd,** gadolinium; **Ho,** holmium; **ICP-MS,** inductively coupled plasma mass spectrometry; **La,** lanthanum; **LMF,** La Meseta Formation; **Lu,** lutetium; **Mn,** manganese; **Nd,** neodymium; **PAAS,** Post-Archean Australian Shale; **Pm,** promethium; **ppm,** parts per million; **Pr,** praseodymium; **REE,** rare earth elements; **RP,** recent penguin; **S,** sample; **Sm,** samarium; **Sr,** strontium; **SMF,** Submeseta Formation; **Tb,** terbium; **Tm,** thulium; **WANT,** West Antarctica; **Y,** yttrium; **Yb,** ytterbium.

TABLE 1 – Samples from the different levels examined in the present contribution.

Sample	Locality	Allomember (level)	Formation	Age
S13	Marambio Island	-	-	Recent
S12	IAA 6/12	Superior (39)	Submeseta	Eocene (Priabonian/Rupelian)
S11	DPV 16/84	Superior (39)	Submeseta	Eocene (Priabonian/Rupelian)
S10	DPV 13/84	Superior (39)	Submeseta	Eocene (Priabonian/Rupelian)
S9	DPV 13/84	Turritella (38)	Submeseta	Eocene (Bartonian)
S8	DPV 13/84	Turritella (38)	Submeseta	Eocene (Bartonian)
S7	IAA 6/12	Turritella (38)	Submeseta	Eocene (Bartonian)
S6	IAA 1/93	Laminado (37)	Submeseta	Eocene (Lutetian)
S5	Cerro Teta	Cucullaea II (36)	La Meseta	Eocene (Ypresian/Lutetian)
S4	IAA 1/90	Cucullaea I (35)	La Meseta	Eocene (middle Ypresian)
S3	Geomarambio	Campamento (34)	La Meseta	Eocene (upper Ypresian)
S2	IAA 1/13	Acantilados II (33)	La Meseta	Eocene (low Ypresian)
S1	64° 15′ 50″ S; 56° 40′ 0″ W	Bahía Pingüino (25)	Cross Valley	Paleocene (Thanetian)

RESULTS

The geochemical signal preserved in the fossil bones of penguins allows us to indirectly understand the changes that occurred in the depositional environment of the analyzed units. The entry of REE into the pore spaces inside the bone tissue of the pieces during the final burial of the pieces, or the very beginning of diagenesis, allows establishment of the chemical variations in the carrier layers of the fossiliferous associations. It is based on chemical elements dissolved in the environmental waters that enter the bone during life, and some modifications can occur in the early stages of diagenesis (Trueman *et al.*, 2006).

ICP-MS analysis

ICP-MS analyses of thirteen samples of recent and fossil penguin bones allow the identification of Ba, Mn, and Sr added to REE concentrations and their distribution (Fig. 3; Tab. 2).

The Sr and Ba concentrations in the vertebrate skeleton vary as a function of the mineral structure, being between 1,200-9,700 ppm and 900-4,000 ppm, respectively; however, it is important to consider that these elements show much lower concentrations in living bones (Trueman & Tuross, 2002). The Sr values of analyzed samples range between 4,210 and 7,198 ppm in fossil bones and record 4,814 ppm in the RP (S13), while Ba varies between 99 and 1,150 ppm in fossils and is 312 ppm in S13; these values are in the same range indicated by Trueman & Tuross (2002). On the other hand, Mn values range between 466–2,388 ppm in fossils, except in S1 and S2 (3,221 and 4,622 ppm, respectively) where they are higher, while it is 1,628 ppm in S13. S1 and S2 samples are also enriched in Ba and show positive anomalies of Eu which can be attributed to some slight modification related to the environmental conditions (*cf.* Shields & Stille, 2001).

The analyzed samples present an average REE concentration of about 700 ppm, which is lower compared with concentrations of REE reported for bones commonly of thousands to tens of thousands ppm (Trueman *et al.*, 2006). Total REE obtained from the RP (S13) is 2,368 ppm, while the other samples are lower compared to S13. The concentrations in the fossil samples vary from 136 to 1,816 ppm with an average of 689 ppm. The REE concentrations in S4, S7, S10, S11, and S12 are very low (130–300 ppm). S6 is the only exception, showing a similar concentration to S13, followed by S2 and S1 (Tab. 2).

The $(La/Sm)_N$ values range from 0.74 to 2.30, with an average value of 1.22 and $(La/Yb)_N$ values range from 0.44 to 1.68 with a mean value of 0.91. S1, S2, S3, S4, S7, S8, S9, S10, and S12 have values of $(La/Yb)_N<1$, as well as the RP (S13). In contrast, $(La/Yb)_N>1$ values are observed for S5, S6, and S11, indicating HREE enrichment (Tab. 2). In the $(La/Sm)_N$ *vs* $(La/Yb)_N$ graph (Fig. 5; *cf.* Trueman *et al.*, 2006) the samples are between groups 2 (S5, S6, S11) and 3, but mostly concentrated in the group 3 (S1, S2, S3, S4, S7, S8, S9, S10 and S12). The RP bone, S13, falls also in field 3. Additionally, all Ce/Ce* values are negative (<1), ranging from 0.34 to 0.89 with an average of 0.66 (Tab. 2), revealing normal oxygenation levels of the paleoenvironment (Shields & Stille, 2001).

The Y/Ho values range from 16 to 40 (28 on average). The Y/Ho ratios allow us to differentiate samples with values lower than 27 (S1, S2, S3, S4, and S6) from those which are over 27 (S7, S8, S9, S10, S11, S12, and S13), the variations of which are considered as being related to changes in parental fluids (Shields & Stille, 2001; Gómez-Peral *et al.*, 2019).

The Eu/Eu* values range from 0.60 to 1.31 (0.94 on average). Eu/Eu* ratios show that S1, S2, S3, and S4 carry positive anomalies (<1; Tab. 2) while they are negative in S5, S6, S7, S8, S9, S10, S11, S12, and S13, but much more pronounced negative anomalies are denoted in the samples of the upper section of the SMF (S9, S10, S11, and S12; Fig. 3), revealing a different behavior from the rest of the samples.

Samples analyzed show REE patterns in the bones of the LMF (S2, S3, S4, and S5 samples; Fig. 3), without notable anomalies and with Eu values slightly lower than PAAS, and they are comparable but mostly lower than the RP (S13). On the other hand, in the overlying SMF the samples can be clearly divided into two groups with markedly different behaviors. The first group includes S6 (basal section) is very similar to the recent bone; S8, S7, and S9 show comparable patterns but are lower than the recent bone (S13). The samples collected from the upper section (S9, S10, S11, and S12) showed marked negative anomalies in Eu (Fig. 3).

TABLE 2 – Trace element contents obtained from the analyzed bones (S1 to S13) added to elemental ratios and anomalies.

Unit	Sample	La	Ce	Pr	Nd	Sm	Eu	Gd	Tb	Dy	Y	Ho	Er	Tm	Yb	Lu	ΣREE	Y/Ho	La/Yb	La/Sm	Ce/Ce*	Eu/Eu*	Ba	Mn	Sr
RP	S13	539.3	694.9	82.8	401.3	99.4	22.8	131.4	22.0	144.4	924.8	31.0	91.9	12.8	81.5	12.4	2,368	29.8	0.49	0.79	0.74	0.94	312	1,628	4,814
SMF	S12	45.2	50.6	5.5	24.7	6.2	0.9	7.8	0.8	7.6	49.0	1.2	4.9	0.2	4.4	0.3	160	39.6	0.75	1.06	0.70	0.61	99	466	2,619
SMF	S11	63.5	40.6	4.5	20.1	4.2	0.6	5.4	0.5	5.7	34.2	0.9	3.6	0.2	3.4	0.2	153	37.7	1.39	2.20	0.47	0.60	312	699	4,483
SMF	S10	31.8	48.5	5.4	23.6	5.2	0.9	6.6	0.7	6.2	33.0	1.0	3.5	0.2	2.9	0.2	137	32.4	0.81	0.88	0.84	0.74	335	1,043	7,198
SMF	S9	102.4	171.5	19.2	79.5	16.7	2.9	20.1	2.5	17.9	111.3	3.4	11.1	1.1	10.0	1.1	460	32.4	0.75	0.89	0.89	0.75	330	2,233	4,845
SMF	S8	91.3	157.2	19.0	80.9	18.0	3.7	21.2	2.8	17.5	90.0	3.3	9.4	1.0	7.4	1.0	433	27.1	0.91	0.74	0.87	0.88	467	1,917	5,782
SMF	S7	69.3	88.1	11.0	45.5	10.5	2.1	12.0	1.6	10.5	62.1	2.0	6.2	0.7	5.8	0.8	266	30.5	0.89	0.96	0.72	0.88	502	815	4,210
SMF	S6	700.0	505.5	58.4	223.6	59.9	13.7	77.7	12.4	71.6	350.2	14.2	38.4	5.2	30.7	4.6	1,816	24.6	1.68	1.70	0.51	0.94	454	2,388	6,968
LMF	S5	342.6	152.0	18.6	78.0	21.6	5.2	28.3	4.9	28.9	177.7	6.6	18.6	3.0	17.3	3.1	729	27.0	1.46	2.30	0.34	0.99	415	1,281	5,158
LMF	S4	54.2	77.3	9.7	38.0	9.0	2.8	12.7	2.9	13.9	87.7	4.0	10.3	2.3	9.2	2.2	249	22.0	0.44	0.87	0.77	1.24	598	1,246	6,159
LMF	S3	182.1	148.0	20.7	83.1	26.0	7.0	30.3	6.1	28.2	142.3	6.9	16.6	3.6	14.1	3.5	576	20.7	0.96	1.02	0.52	1.18	484	1,473	4,303
LMF	S2	565.3	367.8	50.7	192.6	52.7	16.0	72.1	16.8	90.3	541.7	25.3	67.2	14.3	64.9	14.7	1,611	21.4	0.64	1.56	0.45	1.22	1,150	4,622	5,427
CVF	S1	227.3	312.4	36.5	127.8	39.3	12.4	50.3	12.6	51.2	227.9	14.4	31.6	8.5	26.7	8.1	959	15.8	0.63	0.84	0.78	1.31	1,316	3,221	4,979
	RGM-1	7.7	19.6	1.7	6.1	1.4	0.4	1.3	0.2	0.8		0.2	0.5	0.1	0.5	0.1	40.6								

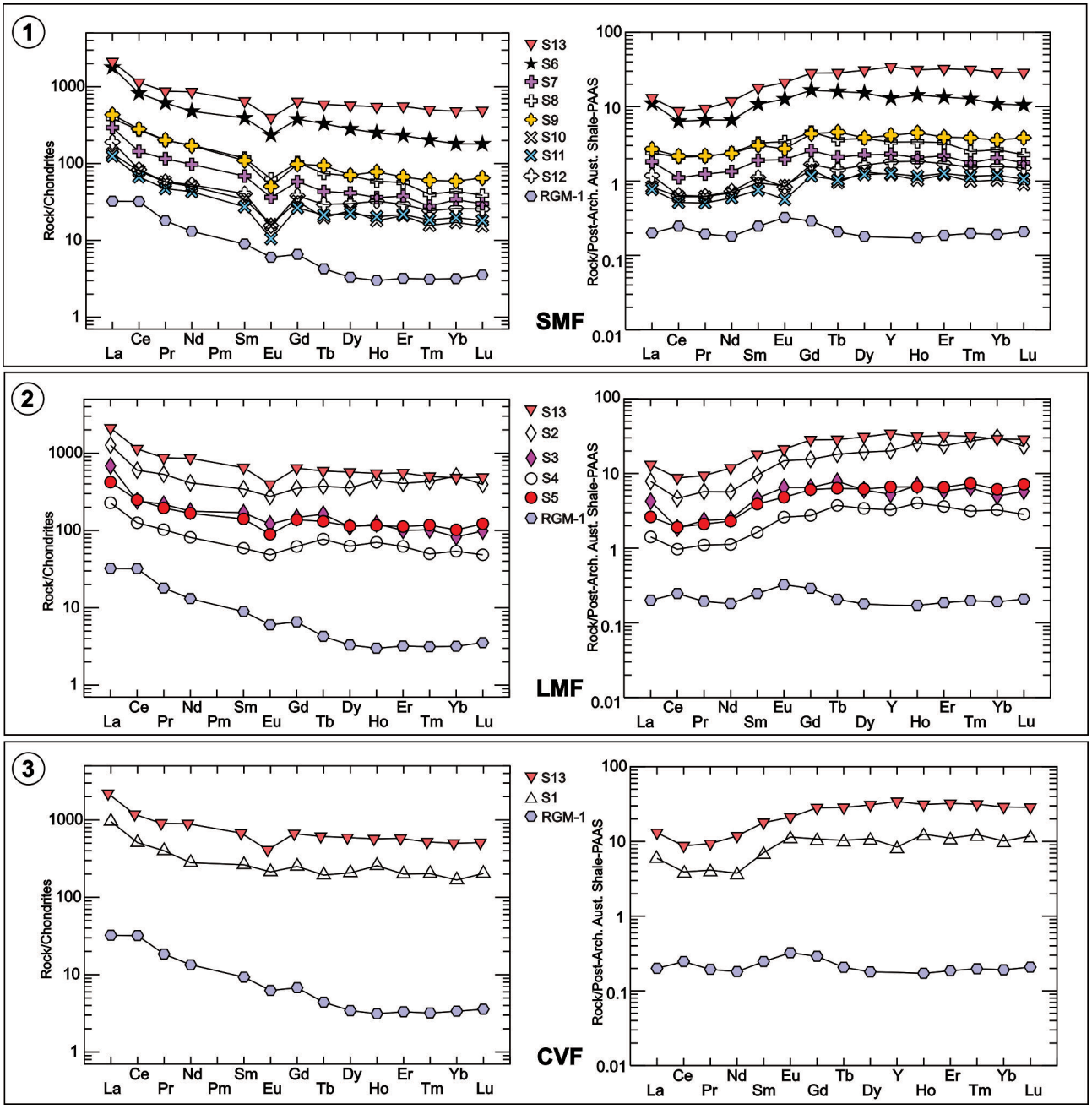

Figure 3. REE values (ppm) from **1, SMF**; **2, LMF**; and **3, CVF**. In all cases, distribution pattern can be compared to RGM-1 and S13 (**RP**). Each plot shows the concentrations normalized to Chondrites (left side; Sun & McDonough, 1989) or to the standard **PAAS** (right side) (McLennan, 1989).

DISCUSSION

The fossil record of Paleogene penguin bones from Seymour Island is abundant and continuous throughout the exposed sections. In general, isolated bones are largely accumulated, whereas skeletons with associated elements are rare (Fig. 4). A single specimen—with associated elements and highly damaged, attributed to weathering and fossil diagenetic fractures (see arrows in Fig. 4.1)—comes from the CVF (Acosta Hospitaleche *et al.*, 2016). Bones collected in the LMF are always found isolated (Fig. 4.2) and many times diagenetically fractured. Finally, the SMF exhibits the complete penguin fossil record. It consists of

partial skeletons, skulls, and articulated limbs, including the exceptional finding of a complete wing covered by its phosphatized skin (Acosta Hospitaleche *et al.*, 2020) (Fig. 4.3).

The REE composition of fossil bones reflects associated water compositions during living, maintaining or not their patterns after the period of recrystallization. The geochemical composition of modern biominerals is frequently used as a fingerprint to identify source locality (*e.g.*, Trueman *et al.*, 2006). Geochemical fingerprinting is based on the observation that the *in vivo* composition of biominerals such as bone and tooth apatite reflects the regional geochemistry (with some variation caused by dietary and metabolic processes during life). Variations in bedrock geology, hydrology, or soil structure may therefore lead to differences in the geochemical composition of biominerals. The REE composition of representative bones that display Eu anomalies supports the hypothesis that REE environmental waters was derived from the breakdown of associated volcaniclastic materials (Trueman *et al.*, 2006).

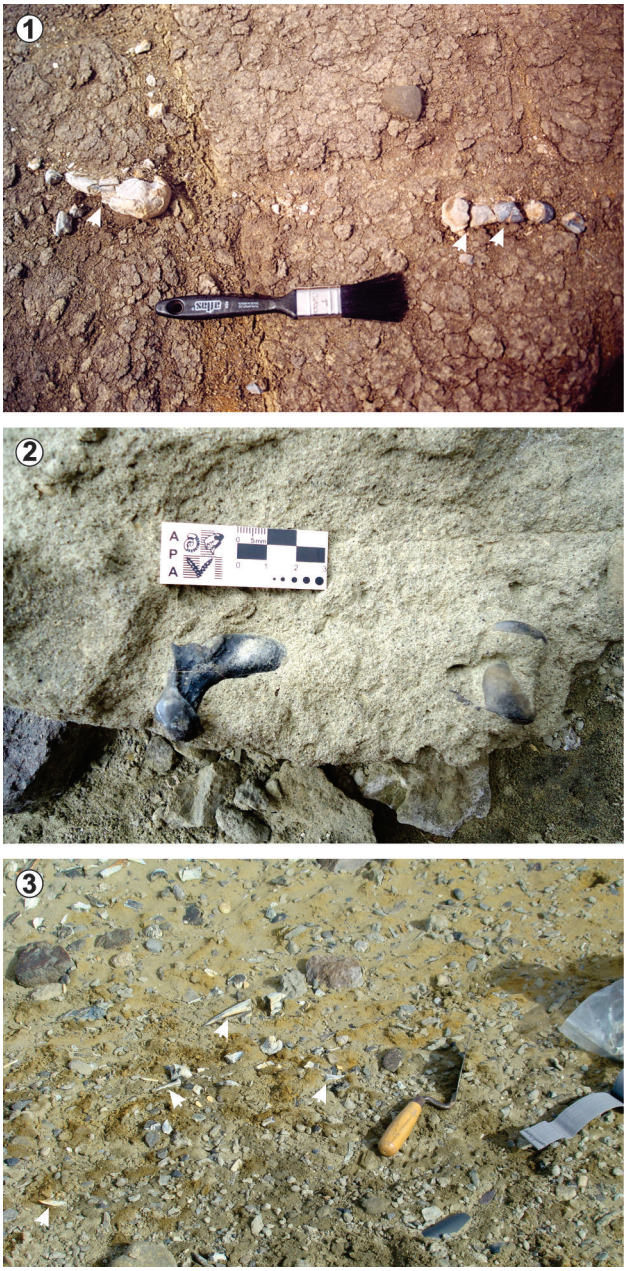

Figure 4. 1–3, Comparison of how penguin fossil fragments are found in the field. **1,** humerus of ***Crossvallia unienwillia*** (Holotype **MLP 00-I-10-1**) fragmented in several pieces in **CVF**, the arrows indicate diagenetic fractures; **2,** femur still in the sandy matrix in **LMF**; **3,** scattered fragments (indicated by white arrows) in the **SMF**.

The geochemical signal preserved in the fossil bones of penguins allows us to recognize the presence or absence of diagenetic alteration and volcanic activity, thus helping us to understand the changes occurring in the depositional environment indirectly. Although recent bones generally show concentrations of REE in the thousands to tens of thousands in ppm (Trueman *et al.*, 2006), total REE concentrations added to Sr and Ba values obtained from samples analyzed in fossil penguin bones are similar to those seen in other unaltered fossil bones regardless of the environmental conditions (*e.g.*, Henderson *et al.*, 1983; Williams, 1988; Janssens *et al.*, 1999; Pike *et al.*, 2002; Trueman & Tuross, 2002). Most samples studied show similar REE pattern distributions, but lower compared with the RP bone (S13; Fig. 3). However, an important distinction can be highlighted from the patterns obtained: bones from LMF show lower values than those of S13 (791 ppm in average; Fig. 3), while samples from the CVF (959 ppm) and especially the SMF show even lower values (268 ppm in average; Tab. 2; Fig. 3), except for S6 which is very similar to S13 (1,816 and 2,368 ppm, respectively) (Tab. 2; Fig. 3).

In addition, ratios of some REE normalized to PAAS as $(La/Yb)_N$ and $(La/Sm)_N$ are used to indicate the nature of fluids related to the environmental context in which they formed (Fig. 4; Trueman *et al.*, 2006; Bosio *et al.*, 2021). In this sense, high $(La/Yb)_N$ ratios, in addition to low $(La/Sm)_N$ ratios have been used as one criterion to indicate late diagenetic recrystallization of biogenic apatite (*e.g.*, Reynard *et al.*, 1999; Trueman *et al.*, 2006; Bosio *et al.*, 2021). This is reinforced by the low contents of Mn related to the absence of

Mn-oxides during the early diagenesis (Tab. 2; *cf.* Bosio *et al.*, 2021). In the studied formations, all samples show a lack of diagenetic alteration in the internal sector of the analyzed bones. Regarding the depositional environment, different geochemical proxies allowed us to interpret changes in environmental conditions. The Ce/Ce* values are negative and compatible with well-oxygenated paleoenvironmental conditions (Shields & Stille, 2001; Gómez-Peral *et al.*, 2014, 2019). Additionally, the $(La/Yb)_N$ *vs.* $(La/Sm)_N$ graphic, shows that the analyzed bones from the LMF and SMF correspond mostly to terrestrial environments (fluvial soils) and subordinately to marine environments (Fig. 5). The Y/Ho ratio is considered a particularly useful monitor for the differentiation between marine and freshwater-influenced deposits (Tostevin *et al.*, 2016; Gómez-Peral *et al.*, 2019 and references therein). Tostevin *et al.* (2016) have recently demonstrated that modern seawater contains Y anomalies (33–40) in near-shore or restricted settings (Tostevin *et al.*, 2016). Particularly, Y/Ho≥30 are used to support preservation of REE and Y patterns in the marine rock record (Tostevin *et al.*, 2016), while other samples showing Y/Ho ratios of ~25 (close to PAAS) denoted a freshwater influence (Gómez-Peral *et al.*, 2019).

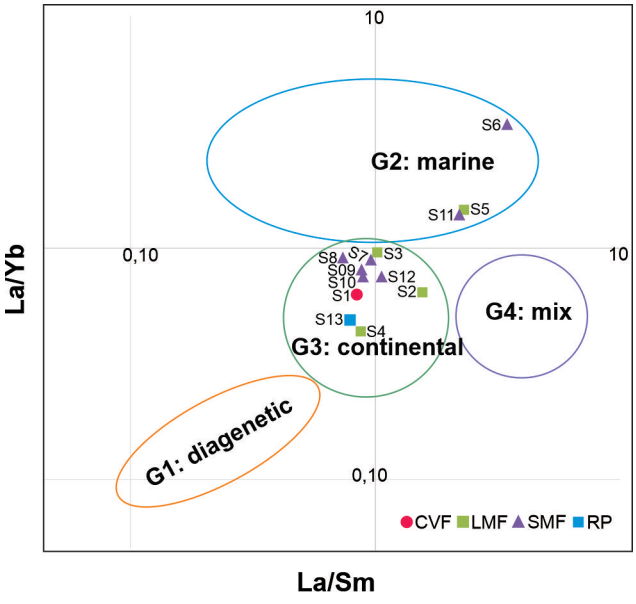

Figure 5. $(La/Yb)_N$ *vs* $(La/Sm)_N$ diagram (from Trueman *et al.*, 2006) showing data obtained from penguin bones from **CVF**, **LMF**, and **SMF**, and from the **RP** bone. Group G1 reflects late diagenetic recrystallization of apatite. Group G2 consists of bones with positive **La/Yb** values related to coastal or shelf marine environments or terrestrial environments with a significant aeolian input. Group G3 is composed of bones with **La/Yb** and **La/Sm**<1, which are related to terrestrial fluvial and soil environments. Group G4 consists of bones lying on a trend line of coincident increase in **La/Sm** values and decrease in **La/Yb** values, typically showing large inter-site variation in mix environments. **RP** (=S13) plots within group 3.

Samples from the SMF show a trend towards more marine conditions according to their higher values of Y/Ho (32 on average; Tab. 2) compared to the lower values obtained from samples of the LMF (Y/Ho of 23 in average; Tab. 2), related to continental freshwater conditions. These agree with paleoenvironmental contexts indicated for each unit, deltaic and estuary deposits for the LMF and shallow marine platform subject to storms for the SMF (Marenssi, 1995; Montes *et al.*, 2019). This reflects the influence of the paleoenvironment on the geochemical variations recorded in these units based on the penguin bones analyzed. In this sense, the high $(La/Yb)_N$ ratios could be associated with littoral-marine to eolic environments (Fig. 5).

Related to the volcanic activity, the REE composition of analyzed bones display negative Eu anomalies (Fig. 3; Tab. 2) supporting that REE in waters could be derived from the interaction with associated volcanic materials (Trueman *et al.*, 2006). The normalized chondrite diagrams show two different provenance signals, probably with volcanic origins reflected in the contribution of Eu (Fig. 3). In this sense, high values of Ba added to positive Eu anomalies, as shown in S1 and S2, point to a possible volcanic influence over the environment (Tostevin *et al.*, 2016). The samples from the upper section of the SMF (S9, S10, S11, and S12) show marked negative Eu anomalies (and lower concentrations of total REE) which can be assumed to be a response to some event of volcanism, such as an orogenic arc. Such a process, which was already operating in the area alongside the fracturing of Gondwana in the Late Cretaceous (Reguero & Goin, 2021), generated a connection between southern South America (Patagonia and Magellanic Regions) and the AP. This connection involved the Weddelian Isthmus associated with an epicontinental sea and occurred towards the late Paleocene (Reguero *et al.*, 2014; Reguero & Goin, 2021).

The negative Eu anomaly found in S9 from the Bartonian, and S10, S11, and S12 from the Priabonian of Seymour Island reflect the regional volcanism to which the region was subjected during the period in which the penguins lived. This volcanism was possibly related to subsidence in the west-

ern margin of the southernmost South American coast and the AP (Jordan *et al.*, 2020). This signal coincides with the final episodes of the opening of the Drake Passage (Fig. 6) during the late Eocene–early Oligocene (~41 to ~27 Ma).

This process was also identified by other proxies, such as the occurrence of ice-rafted debris in levels of the SMF (Doktor *et al.*, 1988). This was interpreted as evidence of a severe climatic deterioration towards the end of the Eocene. It is possible that, for example, valley glaciers were already present in the area by the end of the Eocene. Other cooling signals are provided by a swift decrease of the chemical index alteration values and concomitant inception of illite-dominated clay mineral associations at the top of the SMF. This suggests a transition to cold, frost-prone, and relatively dry conditions during the late Eocene (Ivany *et al.*, 2006). Likewise, the decrease in leaf size recorded in this unit suggests that the climate deteriorated towards the end of the Eocene (Case, 1988; Reguero *et al.*, 2002, 2013). The shift from cool, temperate, humid Valdivian-type forest to more impoverished vegetation was accompanied by a decrease in typical Eocene dinoflagellate cysts, an increase in sea ice-indicative marine phytoplankton, and an increase in reworked palynomorphs. All these point toward the onset of periglacial conditions and a subpolar climate in the back-arc James Ross Basin just before the Eocene/Oligocene boundary (Warny *et al.*, 2018).

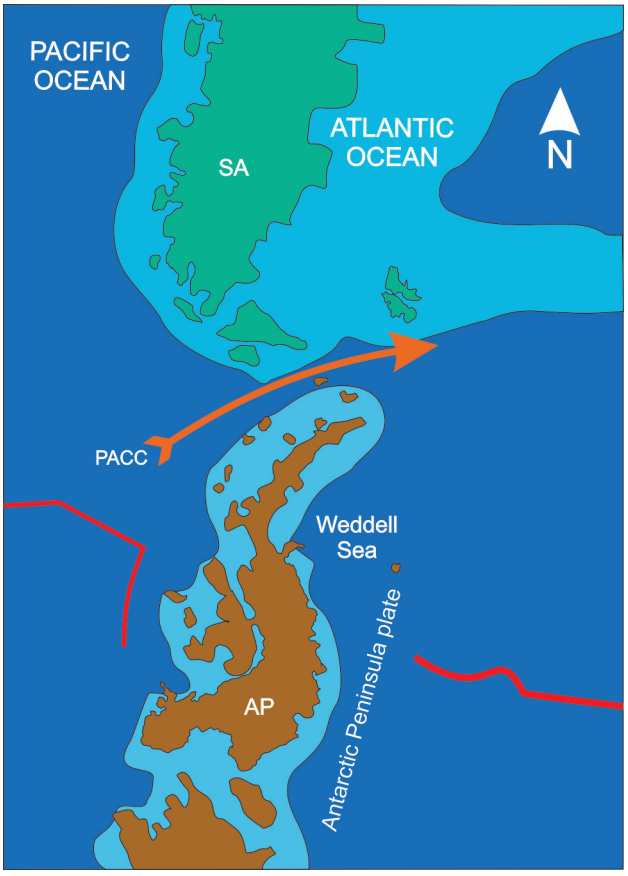

Figure 6. The evolution of the Drake Passage region (~43 Ma; modified from Reguero & Goin, 2021) based on Brown *et al.* (2006); red lines are spreading ridges. Abbreviations: **PACC;** Proto-Atlantic Circumpolar Current; **SA,** South America.

The tectonic episodes described above could also be identified by examining equivalent samples from the southernmost tip of South America. For instance, the negative Eu anomaly found in the Bartonian and Priabonian samples should be detected in penguin bones from the Leticia Formation in the Austral Basin of Tierra del Fuego (Acosta Hospitaleche & Olivero, 2016; Olivero *et al.,* 2020) and in the Eocene of the Loreto, Río Turbio, and Río Baguales formations in the Magallanes Region of Chile (Sallaberry *et al.*, 2010).

CONCLUSIONS

Although some taphonomical differences between the fossil penguins from the unit could be observed, the preservation degree is good enough along the whole sequence to perform a geochemical analysis on these bones. The geochemical signal preserved in these fossils allows us to recognize the degree of diagenetic alteration (fossil-diagenesis of bones), the influence of volcanic activity, and indirectly understand the changes that have occurred in the depositional environment. Summarizing, the main conclusions of the present research can be pointed out:

Through the interpretation of ratios of $(La/Yb)_N$ and $(La/Sm)_N$ and contents of Mn, it was possible to conclude that all the samples (penguin bones) included in this study showed absence of diagenetic alteration.

The Ce/Ce* values recorded are compatible with well oxygenated paleoenvironmental conditions. Additionally, and concurring with the previous sedimentological analyses, the $(La/Yb)_N$ *vs.* $(La/Sm)_N$ graphic and Y/Ho values indicate that the samples from the LMF show less marine affinity than those from the SMF.

The REE patterns of the analyzed bones, comparable to

living bones, displayed negative Eu anomalies, supporting that REE in environmental waters could be derived from the breakdown of associated volcaniclastic materials. The samples from the upper section of the SMF (S9, S10, S11, and S12) present marked negative Eu anomalies and the lowest concentrations of total REE, which can be assumed as a response to some event of volcanic activity, such as an orogenic arc.

This signal coincides in time with the opening of the Drake Passage and with the tectonic changes occurring between the end of the Eocene and the beginning of the Oligocene as a result of the subsidence in the western margin of South American and AP coasts.

ACKNOWLEDGEMENTS

The authors would like to thank Dr. M. Griffin for reading the text article. To the Instituto Antártico Argentino (Dirección Nacional del Antártico) for funding the fieldwork. To Centro de Investigaciones Geológicas (CIG-CONICET), Agencia Nacional de Promoción Científica y Tecnológica (PICT 2017 0607), Consejo Nacional de Investigaciones Científicas y Técnicas (PIP 0096), Universidad Nacional de La Plata (PI N953, N955) and Oceanwide Expeditions, Vlissingen [NI], for partially supporting the research. To the anonymous reviewers, Manuel Montes, and the editorial committee of PE-APA for their suggestions and comments.

REFERENCES

Acosta Hospitaleche, C., De los Reyes, M., Santillana, S., & Reguero, M. (2020). First fossilized skin of a giant penguin from the Eocene of Antarctica. *Lethaia*, *53*(3), 409–420. https://doi.org/10.1111/let.12366

Acosta Hospitaleche, C., Haidr, N., Paulina Carabajal, A., & Reguero, M. (2019b). First skull of *Anthropornis grandis* associated with postcranial elements. *Comptes Rendus Palevol*, *18*(6), 99–617. https://doi.org/10.1016/j.crpv.2019.06.003

Acosta Hospitaleche, C., Jadwiszczak, P., Clarke, J., & Cenizo, M. (2019a). The fossil record of birds from the James Ross Basin, West Antarctica. *Advances in Polar Sciences*, *30*(3), 251–273. http://dx.doi.org/10.13679/j.advps.2019.0014

Acosta Hospitaleche, C. & Olivero, E. (2016). Re-evaluation of the fossil penguin *Palaeeudyptes gunnari* from the Eocene Leticia Formation, Argentina: Additional material, systematics and palaeobiology. *Alcheringa*, *40*(3), 373–382. https://doi.org/10.1080/03115518.2016.1144994

Acosta Hospitaleche, C., Pérez, L. M., Marenssi, S., & Reguero, M. (2016). Taphonomic analysis and paleobiological observation of *Crossvallia unienwillia* Tambussi *et al.* 2005: significance of the oldest penguin record of Antarctica. *Ameghiniana*, *53*(3), 282–295. https://doi.org/10.5710/AMGH.24.08.2015.2917

Acosta Hospitaleche, C. & Reguero, M. (2010). First articulated skeleton of *Palaeeudyptes gunnari* from the late Eocene of Seymour (= Marambio) Island (Antarctica). *Antarctic Sciences*, *22*(3), 289–298. https://doi.org/10.1017/S0954102009990769

Acosta Hospitaleche, C. & Reguero, M. (2014). *Palaeeudyptes klekowskii*, the most complete penguin skeleton found in the Eocene of Antarctica: taxonomic remarks. *Geobios*, *47*(3), 77–85. https://doi.org/10.1016/j.geobios.2014.03.003

Acosta Hospitaleche, C., Reguero, M., & Scarano, A. (2013). Main pathways in the evolution of Antarctic fossil penguins. *Journal of South American Earth Sciences*, *43*, 101–111. https://doi.org/10.1016/j.jsames.2013.01.006

Andersson, J. G. (1906). On the geology of Graham Land. *Bulletin of the Geological Institution of the University of Upsala*, *7*, 19–71.

Bibby, J. (1966). The stratigraphy of part of north-east Graham Land and the James Ross Island group. *British Antarctic Survey Scientific Reports*, *53*, 1–37.

Blokland, J. C., Reid, C. M., Worthy, T. H., Tennyson, A. J. D., Clarke, J. A., & Scofiel, R. P. (2019). Chatham Island Paleocene fossils provide insight into the palaeobiology, evolution, and diversity of early penguins (Aves, Sphenisciformes). *Palaeontologia Electronica*, 22.3.78. https://doi.org/10.26879/1009

Bosio, G., Gioncada, A., Gariboldi, K., Bonaccorsi, E., Collareta, A., Pasero, M., Di Celma, C., Malinverno, E., Urbina, M., & Bianucci, G. (2021). Mineralogical and geochemical characterization of fossil bones from a Miocene marine Konservat-Lagerstätte. *Journal of South American Earth Sciences*, *105*, 102924. https://doi.org/10.1016/j.jsames.2020.102924

Brown, B., Gaina, C., & Müller, D. (2006). Circum-Antarctic palaeobathymetry: Illustrated examples from Cenozoic to recent times. *Palaeogeography, Palaeoclimatolgy, Palaeoecolgy*, *231*, 158–168. https://doi.org/10.1016/j.palaeo.2005.07.033

Case, J. (1988). Paleogene floras from Seymour Island, Antarctic Peninsula. In R. M. Feldmann & M. O. Woodburne (Eds.), *Geology and paleontology of Seymour Island, Antarctica Peninsula* (pp. 523–530). Geological Society of America Memoir.

Cook, P. J. & Shergold, J. H. (2005). *Phosphate Deposits of the World. Proterozoic and Cambrian Phosphorites, vol. 1*. Cambridge University Press.

Crame, J. A., Beu, A. G., Ineson, J. R., Francis, J. E., Whittle, R. J., & Bowman, V. C. (2014). The early origin of the Antarctic Marine Fauna and its evolutionary implications. *PLoS One*, *9*(12), e114743. https://doi.org/10.1371/journal.pone.0114743

De Baar, H. J., Bacon, M. P., Brewer, P. G., & Bruland, K. W. (1985). Rare earth elements in the Pacific and Atlantic Oceans. *Geochimica et Cosmochimica Acta*, *49*(9), 1943–1959.

Decrée, S., Herwartz, D., Mercadier, J., Miján, I., de Buffrénil, V., Leduc, T., & Lambert, O. (2018). The post-mortem history of a bone revealed by its trace element signature: the case of a fossil whale rostrum. *Chemical Geology*, *477*, 137–150. https://doi.org/10.1016/j.chemgeo.2017.12.021

Doktor, M., Gaździcki, A., Marenssi, S. A., Porebski, S. J., Santillana, S. N., & Vrba, A. V. (1988). Argentine-Polish geological investigations on Seymour (Marambio) Island, Antarctica, 1988. *Polish Polar Research*, *9*(4), 521–141.

Eagles, G. & Jokat, W. (2014). Tectonic reconstructions for paleobathymetry in Drake passage. *Tectonophysics*, *611*, 28–50. https://doi.org/10.1016/j.tecto.2013. 11.021

Eagles, G., Livermore, R. A., Fairhead, J. D., & Morris, P. (2005). Tectonic evolution of the west Scotia Sea. *Journal of Geophysical Research*, *11*, B02401. http://dx.doi.org/10.1029/2004JB003154

Eagles, G., Livermore, R., & Morris, P. (2006). Small basins in the Scotia Sea: The Eocene Drake passage gateway. *Earth and Planetary Science Letters*, *242*(3–4), 343–353. https://doi.org/10.1016/j.epsl.2005.11.060

Elliot, D. H., Rinaldi, C. A., Zinsmeister, W., Trautman, T. A., Bryant, W. A., & Del Valle, R. A. (1975). Geological investigations on Sey-

mour Island, Antarctic Peninsula. *Antarctic Journal of the United States*, *10*(4), 182–186.

Elliot, D. H. & Trautman, T. A. (1982). Lower Tertiary strata on Seymour Island, Antarctic Peninsula. In C. Craddock (Ed.), *Antarctic Geoscience* (pp. 287–297). University of Wisconsin Press.

Feldman, R. & Woodbume, M. (1988). *Geology and Paleontology of Seymour Island, Antarctic Peninsula.* Geological Society of America Memoir 169. https://doi.org/10.1130/MEM169

Fretzdorff, S., Worthington, T. J., Haase, K. M., Hekinian, R., Franz, L., Keller, R. A., & Stoffers, P. (2004). Magmatism in the Bransfield Basin: Rifting of the South Shetland Arc? *Journal of Geophysical Research*, *109*(B12208), 1–19. https://doi.org/10.1029/2004JB003046

Gómez-Peral, L. E., Arrouy, M. J., Poiré, D. G., & Cavarozzi, C. E. (2019). Redox-sensitive element distribution in the Neoproterozoic Loma Negra Formation in Argentina, in the Clymene Ocean context. *Precambrian Research*, *332*, 105384. https://doi.org/10.1016/j.precamres.2019.105384

Gómez-Peral, L. E., Kaufman, A. J., & Poiré, D. G. (2014). Paleoenvironmental implications of two phosphogenic events in Neoproterozoic sedimentary successions of the Tandilia System, Argentina. *Precambrian Research*, *252*, 88–106. https://doi.org/10.1016/j.precamres.2014.07.009

Henderson, P., Marlow, C. A., Molleson, T. I., & Williams, C. T. (1983). Patterns of chemical change during bone fossilization. *Nature*, 306(5941), 358–360. https://doi.org/10.1038/306358a0

Herwartz, D., Tütken, T., Münker, C., Jochum, K. P., Stoll, B., & Sander, P. M. (2011). Timescales and mechanisms of REE and Hf uptake in fossil bones. *Geochimica et Cosmochimica Acta*, *75*(1), 82–105. https://doi.org/10.1016/j.gca.2010.09.036

Hombron, J. B. & Jacquinot, H. (1841). Description de plusieurs oiseaux nouveaux ou peu connus, provenant de l'expedition autour du monde faite sur les corvettes l'Astrolabe et la Zelee. *Annales des sciences naturelles*, *16*(2), 312–320.

Ivany, L., van Simaeys, S., Domack, E., & Samson, S. (2006). Evidence for an earliest Oligocene ice sheet on the Antarctic Peninsula. *Geology*, *34*(5), 377–380.

Janssens, K., Vincze, L., Vekemans, B., Williams, C. T., Radke, M., Haller, M., & Knochel, A. (1999). The non-destructive determination of REE in fossilized bone using synchrotron radiation induced K-line X-ray microflourescence analysis. *Fresenius Journal of Analytical Chemistry*, *363*(4), 126–413. https://doi.org/10.1007/s002160051212

Jordan, T. A., Riley, T. R., & Siddoway, C. S. (2020). The geological history and evolution of West Antarctica. *Nature Reviews Earth & Environment*, *1*(2), 117–133. https://doi.org/10.1038/s43017-019-0013-6

Lagabrielle, Y., Goddéris, Y., Donnadieu, Y., Malavieille, J., & Suarez, M. (2009). The tectonic history of Drake Passage and its possible impacts on global climate. *Earth Planetary Science Letters*, *279*(3–4), 197–211. https://doi.org/10.1016/j.epsl.2008.12.037

Lawrence, M. G., Kenneth, A. G., Collerson, D., & Kamber, B. S. (2006). Direct quantification of rare earth element concentrations in natural waters by ICP-MS. *Applied Geochemistry*, *21*(5), 839–848. https://doi.org/10.1016/j.apgeochem.2006.02.013

Lawver, L. A. & Gahagan, L. M. (2003). Evolution of Cenozoic seaways in the circum-Antarctic region. *Palaeogeography, Palaeoclimatology, Palaeoecology*, *198*(1–2), 11–37. https://doi.org/10.1016/S0031-0182(03)00392-4

Livermore, R., Nankivel, A., Eagles, G., & Morris, P. (2005). Paleogene opening of Drake passage. *Earth Planetary Science Letters*, *236*(1–2), 459–470. https://doi.org/10.1016/j.epsl.2005.03.027

MacDonald, D. I. M., Baker, P. F. Garrett, S. W., Ineson, J. R., Pirrie, D., Storey, B. C., Whitham, A. G., Kinghorn, R. R. F., & Marshall, J. E. A. (1988). A preliminary assessment of the hydrocarbon potential of the Larsen Basin, Antarctica. *Marine and Petroleoum Geology*, *5*(1), 34–53. https://doi.org/10.1016/0264-8172 (88)90038-4

Macellari, C. E. (1988). Stratigraphy, sedimentology and paleoecology of Upper Cretaceous/Paleocene shelf deltaic sediments of Seymour Island. In R. M. Feldmann & M. O. Woodburne (Eds.), *Geology and paleontology of Seymour Island, Antarctic Peninsula* (pp. 25–53). Geological Society of America Memoir.

Marenssi, S. A. (1995). *Sedimentología y paleoambientes de sedimentación de la Formación La Meseta, Isla Marambio, Antártica.* [PhD Thesis, Facultad de Ciencias Exactas y Naturales, Universidad de Buenos Aires]. Retrieved from https://bibliotecadigital.exactas.uba.ar/download/tesis/tesis_n2775_Marenssi.pdf

Marenssi, S. A. & Elliot, D. H. (1992). The Paleogene of the James Ross Basin, Antarctica. *Simposio Paleógeno de Sudamérica* (Abstracts n° 26). Punta Arenas.

Marenssi, S. A., Net, L. I., & Santillana, S. N. (2002). Provenance, environmental and paleogeographic controls on sandstone composition in an incised-valley system: The Eocene La Meseta Formation, Seymour Island, Antarctica. *Sedimentary Geology*, *150*(3–4), 301–321. https://doi.org/10.1016/S0037-0738(01)00201-9

Marenssi, S. A. & Santillana, S. N. (1994). Unconformity-bounded units within the La Meseta Formation, Seymour Island, Antarctica: a preliminary approach. *Abstracts of the 21° Polar Symposium* (pp. 33–37). Warszawa.

Marenssi, S. A., Santillana, S. N., & Bauer, M. (2012). Estratigrafía, petrografía sedimentaria y procedencia de las formaciones Sobral y Cross Valley (Paleoceno), Isla Marambio (Seymour), Antártica. *Andean Geology*, *39*(1), 67–91.

Marenssi, S. A., Santillana, S. N., & Rinaldi, C. A. (1998). Stratigraphy of the La Meseta Formation (Eocene), Marambio (Seymour) Island, Antarctica. *Publicación Especial de la Asociación Paleontológica Argentina*, *5*, 137–146.

McLennan, S. M. (1989). Rare earth elements in sedimentary rocks: influence of provenance and sedimentary processes. *Reviews in Mineralogy & Geochemistry*, 21, 169–200.

Montes, M., Nozal, F., Olivero, E., Gallastegui, G., Santillana, S., Maestro, A., López Martínez, J., González, L., & Martín-Serrano, A. (2019). *Geología y Geomorfología de isla Marambio (Seymour) 1:20.000.* Instituto Geológico y Minero de España.

Montes, M., Nozal, F., Santillana, S. N., Marenssi, S. A., & Olivero, E. (2013). *Mapa geológico 1:20000 de la Isla Marambio (Seymour).* Instituto Geológico y Minero de España and Instituto Antártico Argentino.

Montes, M., Nozal, F., Santillana, S. N., Marenssi, S. A., Olivero, E. B., & Maestro, A. (2008). Mapa geológico 1:20.000 de la isla Marambio (mar de Weddell, Antártida). Congreso Geológico de España, N° 7, Las Palmas. *Geotemas*, *10*, 709–712.

Montes, M., Santillana, S. N., Nozal, F., & Marenssi, S. A. (2007). Secuencias de relleno del valle incidido en la Formación Cross Valley. Paleoceno superior de la isla Marambio (Mar de Weddell, Antártica). *Abstracts of the 6° Simposio Argentino y Latinoamericano sobre Investigaciones* (GEORE830). Buenos Aires.

Olivero, E. B., Ponce, J. J., & Martinioni, D. R. (2008). Sedimentology and architecture of sharp-based tidal sandstones from the Upper Marambio Group, Maastrichtian of Antarctica. *Sedimentary Geology*, *210*(1–2), 11–26. https://doi.org/10.1016/j.sedgeo.2008.07.003

Olivero, E. B., Torres Carbonell, P. J., Svojtka, M., Fanning, M., Hervé, F., & Nývlt, D. (2020). Eocene volcanism in the Fuegian Andes: Evidence from petrography and detrital zircons in marine volcaniclastic sandstones. *Journal of South American Earth Sciences*, *104*, 102853. https://doi.org/10.1016/j.jsames.2020.102853

Pike, A. W. G., Hedges, R. E. M., & Van Calsteren, P. (2002). U-series dating of bone using the diffusion–adsorption model. *Geochimica et Cosmochimica Acta*, *66*(24), 4273–4286. https://doi.org/10.1016/S0016-7037(02)00997-3

Presslee, S., Penkman, K., Fischer, R., Slidel-Richards, E., Southon, J., Acosta Hospitaleche, C., Collins, M., & MacPhee, R. (2020). Assessment of different screening methods for selecting palaeontological bone samples for peptide sequencing. *Journal of Proteomics*, *230,* 103986. https://doi.org/10.1016/j.jprot.2020.103986

Reguero, M. A., Gelfo, J. N., López, G. M., Bond, M., Abello, A., Santillana, S. N., & Marenssi, S. A. (2014). Final Gondwana breakup: The Paleogene South American native ungulates and the demise of the South America–Antarctica land connection. *Global and Planetary Change*, *123*(Part B), 400–413. https://doi.org/10.1016/j.gloplacha.2014.07.016

Reguero, M. A. & Goin, F. J. (2021). Paleogeography and biogeography of the Gondwanan final breakup and its terrestrial vertebrates: New insights from southern South America and the "double Noah's Ark" Antarctic Peninsula. *Journal of South American Earth Sciences*, *108*, 103358. https://doi.org/10.1016/j.jsames.2021.103358

Reguero, M., Goin, F., Acosta Hospitaleche, C., Dutra, T., & Marenssi, S. (2013). Paleogene terrestrial vertebrates of the James Ross basin. In M. Reguero, F. Goin, C. Acosta Hospitaleche, T. Dutra & S. Marenssi (Eds.), *Late Cretaceous/Paleogene West Antarctica Terrestrial Biota and its Intercontinental Affinities* (pp. 74–88). Springer Dordrecht.

Reguero, M. A., Marenssi, S. A., & Santillana, S. N. (2002). Antarctic Peninsula and South America (Patagonia) Paleogene terrestrial faunas and environments: biogeographic relationships. *Palaeogeography, Palaeoclimatology, Palaeoecolgy*, *179*(3–4), 189–210. https://doi.org/10.1016/S0031-0182(01)00417-5

Reynard, B., Lécuyer, C., & Grandjean, P. (1999). Crystal–chemical controls on rare-earth element concentrations in fossil biogenic apatites and implications for paleoenvironmental reconstructions. *Chemical Geology*, *155*(3–4), 233–241. https://doi.org/10.1016/S0009-2541(98)00169-7

Rinaldi, C. A., Massabie, A., Morelli, J., Rosenman, L. H., & Del Valle, R. A. (1978). Geología de la isla Vicecomodoro Marambio, Antártica. *Contribución Instituto Antártico Argentino*, *217*, 1–37.

Sadler, P. M. (1988). Geometry and stratification of uppermost Cretaceous and Paleogene units on Seymour Island, northern Antarctic Peninsula. In R. M. Feldman & M. O. Woodburne (Eds.), *Geology and Paleontology of Seymour Island, Antarctic Peninsula* (pp. 303–320). Geological Society of America Memoir 169.

Sallaberry, M. A., Yury-Yáñez, R. E., Otero, R. A., Soto-Acuña, S., & Torres, T. (2010). Eocene birds from the western margin of southernmost South America. *Journal of Paleontology*, *84*(6), 1061–1070. https://doi.org/10.1666/09-157.1

Shields, G. & Stille, P. (2001). Diagenetic constraints on the use of cerium anomalies as palaeoseawater redox proxies: an isotopic and REE study of Cambrian phosphorites. *Chemical Geology*, *175*(1–2), 29–48. https://doi.org/10.1016/S0009-2541(00)00362-4

Sijp, W. P. & England, M. H. (2004). Effect of the Drake Passage through flow on global climate. *Journal of Physical Oceanography*, *34*, 1254–1266. https://doi.org/10.1175/1520-0485(2004)034<1254:EOTDPT>2.0.CO;2

Slack, K. E., Jones, C. M., Ando, T., Harrison, G. L., Fordyce, R. E., Arnason, U., & Penny, D. (2006). Early penguin fossils, plus mitochondrial genomes, calibrate avian evolution. *Molecular biology and evolution*, *23*(6), 1144–1155. https://doi.org/10.1093/molbev/msj124

Sun, S. S. & McDonough, W. F. (1989). Chemical and isotopic systematics of oceanic basalts; implications for mantle composition and processes. In A. D. Saunders & M. J. Norry (Eds.), *Magmatism in the ocean basins* (pp. 313–345). Geological Society of London 42.

Tambussi, C. P., Reguero, M. A., Marenssi, S. A., & Santillana, S. N. (2005). *Crossvallia unienwillia*, a new Spheniscidae (Sphenisciformes, Aves) from the Late Paleocene of Antarctica. *Geobios*, *38*(5), 667–675. https://doi.org/10.1016/j.geobios.2004.02.003

Taylor, S. R. & McLennan, S. M. (1985). *The Continental Crust: Its Composition and Evo-lution*. Blackwell Scientific.

Toggweiler, J. R. & Bjornsson, H. (2000). Drake passage and paleoclimate. *Journal of Quaternary Science*, *15*(4), 319–328.

Tostevin, R., Shields, G. A., Tarbuck, G. M., He, T., Clarkson, M. O., & Wood, R. A. (2016). Effective use of cerium as redox proxy in carbonate-dominated marine settings. *Chemical Geology*, *438*, 146–162. https://doi.org/10.1016/j.chemgeo.2016.06.027

Trueman, C. N., Behrensmeyer, A. K., Potts, R., & Tuross, N. (2006). High-resolution records of location and stratigraphic provenance from the rare earth element composition of fossil bones. *Geochimica et Cosmochimica Acta*, *70*(17), 4343–4355. https://doi.org/10.1016/j.gca.2006.06.1556

Trueman, C. N. & Tuross, N. (2002). Trace metals in recent and fossil bone. In M. J. Kohn, J. J. Rakovan, & J. M. Hughes (Eds.), *Phosphates: geochemical, geobiological, and materials importance* (pp. 489–521). Reviews in Mineralogy and Geochemistry.

Warny, S., Kymes, C. M., Askin, R., Krajewski, K., & Tatur, A. (2018). Terrestrial and marine floral response to latest Eocene and Oligocene events on the Antarctic Peninsula. *Palynology*, *43*(1), 4–21. https://doi.org/10.1080/01916122.2017.1418444

Williams, C. T. (1988). Alteration of chemical composition of fossil bones by soil processes and groundwater. In G. Grupe & B. Herrmann (Eds.), *Trace Elements in Environmental History* (pp. 27–40). Springer-Verlag. https://doi.org/10.1007/978-3-642-73297-3_3

Williams, T. D. (1995). *The Penguins, Spheniscidae*. Oxford University Press.

Zinsmeister, W. J. (1982) Late Cretaceous-Early Tertiary molluscan biogeography of southern Circum-Pacific. *Journal of Paleontology*, *56*(1), 84–102.

doi: 10.5710/PEAPA.14.11.2022.443

Recibido: 16 de septiembre 2022
Aceptado: 14 de noviembre 2022
Publicado: 22 de febrero 2023